



Proceedings of the Sixth International Conference on
Railway Technology: Research, Development and Maintenance
Edited by: J. Pombo
Civil-Comp Conferences, Volume 7, Paper 18.6
Civil-Comp Press, Edinburgh, United Kingdom, 2024
ISSN: 2753-3239, doi: 10.4203/ccc.7.18.6
©Civil-Comp Ltd, Edinburgh, UK, 2024

Suppressing Track Lateral Misalignment at High Temperatures by Focusing on Unsupported Sleepers

M. Kusuda

**Track and Structures Engineering Office, Track and Structures
Department, Railway Operations Headquarters, West Japan
Railway Company
Osaka, Japan**

Abstract

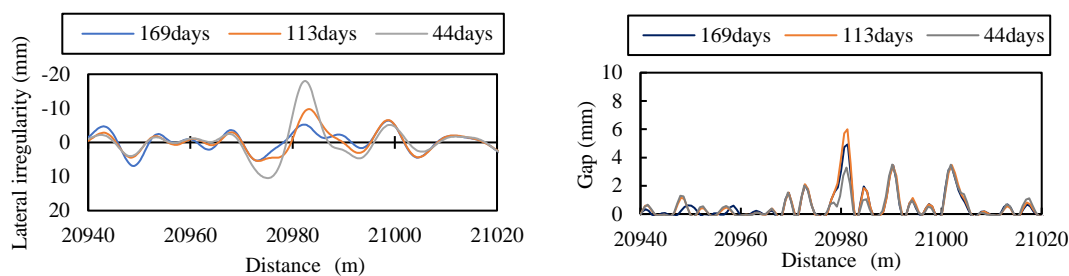
The design and management of ballasted track assume that the track panel is uniformly supported. As an actual situation, unsupported sleepers which are not supported on the ballast in the case where the train load does not act on them, are found sporadically at ballasted track. Unsupported sleepers are known to cause management problems such as loss of track buckling stability. In fact, continuous unsupported sleepers have been found to be present in all locations where track has been abnormally misaligned during high-temperature periods. In this study, a numerical analysis was performed on buckling stability, and the limit of lateral axle force to prevent shifting of track, in consideration of the actual situation of unsupported sleepers. As a result, it has become clear that the presence of unsupported sleepers increases track lateral displacement when the rail temperature increases, and that to ensure the lateral stability of the track at locations where unsupported sleepers exist, it is necessary to keep track lateral irregularity to a small level. Based on the results, management standards for unsupported sleepers and lateral track irregularity at high temperatures were established, and have been put into operation, and are proving effective.

Keywords: ballasted track, unsupported sleeper, track stability, track irregularity, lateral axle force, management standard.

1 Introduction

Unsupported sleepers are found sporadically at railway ballasted tracks, and the support state of sleepers is not necessarily uniform. Unsupported sleepers cause various problems in track geometry management. The authors [1],[2] have proposed a method for detecting unsupported sleepers easily and accurately using track specifications and level track irregularity data measured by track geometry vehicle. By comparing the gap between the top surface of the ballast bed and the bottom surface of the unsupported sleeper (hereinafter referred to as gap) calculated using this method with the gap measured on site, it was confirmed that good estimation accuracy could be obtained for CWR sections. In addition, using actual data from the commercial lines, the relationship between the occurrence of unsupported sleepers, sleeper spacing, and irregularity of longitudinal level surface, and clarified the effect of the occurrence of unsupported sleepers on load distribution during vehicle running has been clarified. By considering the existence of unsupported sleepers, it is possible to understand the rail seat load that each sleeper supports and enable a detailed assessment of the lateral stability of the track, which plays an important role in vehicle running safety.

Once again, the locations where significant lateral track misalignments that have occurred in recent years have caused transportation problems were investigated. An example of the results is shown in Figure 1. Here, the legend indicates the number of days back from the date the event occurred, and the location of event is 20980 m. It was found that the lateral irregularity was gradually progressing at that point, that the unsupported sleepers were continuously present, that the gaps were gradually increasing, and that the continuous unsupported sections were expanding. The reason why the gap 44 days ago became smaller is because the tamping operation was carried out 49 days before the event occurred.



[a] Lateral irregularity

in 10m chord versine method

[b] Gap

Figure 1: Example of changes in track conditions at transportation problem.

Therefore, with the aim of preventing such incidents from occurring in the future, an investigation was conducted into the relationship between rail temperature increase and lateral deformation of the track, as well as the limit of lateral axle force, based on the actual situation of unsupported sleepers. Based on these survey results, maintenance standards that can be implemented at maintenance field office were proposed. Furthermore, the remaining issues are mentioned.

2 Methods

2.1 Calculation method for unsupported sleepers

The gap is determined using the method described in References [1],[2]. Specifically, as shown in Figure 2, the restored waveform estimated from the dynamic longitudinal level irregularity is used as the vertical uneven shape of the upper surface of the track-bed in the longitudinal direction of the rail (hereinafter referred to as “track-bed surface shape”). By calculating the difference between the deflection shape of the track panel and the track-bed surface shape when no train load is applied, it is possible to calculate the gap that represents the distance between the track and the track-bed surface shape at each sleeper.

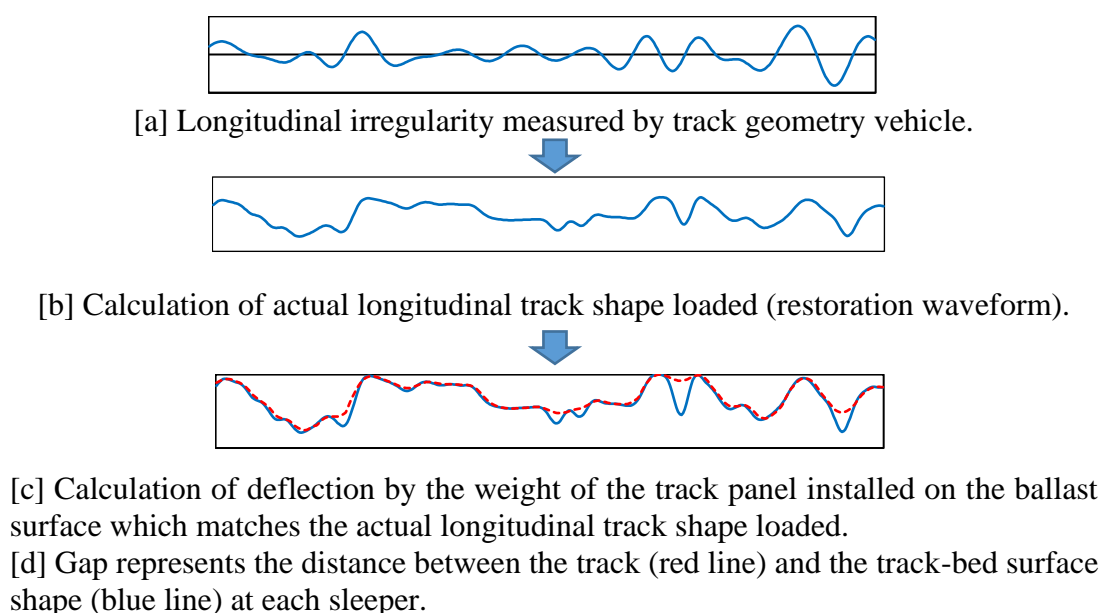
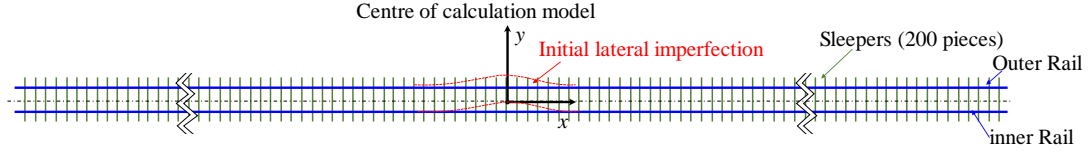


Figure 2: Flow of gap calculation of unsupported sleeper

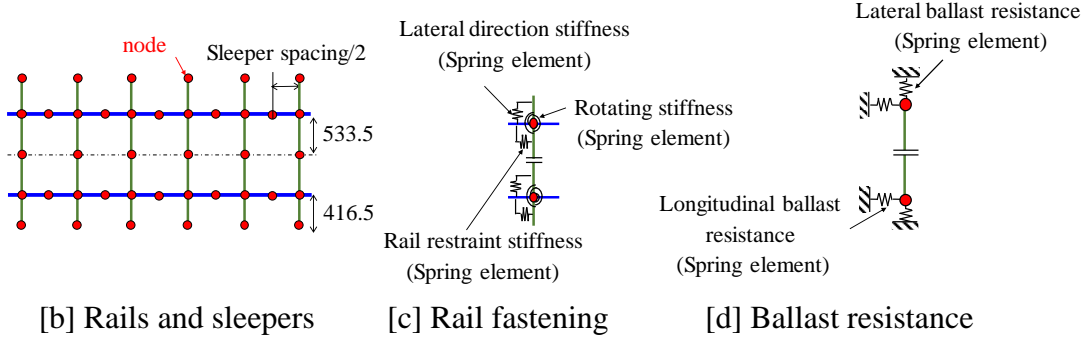
2.2 Method for estimating track lateral shift due to increase in rail temperature

Perform balance calculations when a temperature rise is applied to a finite element model expressed by spring elements and beam elements. The analysis model is shown in Figure 3. It allows track specifications such as track bed lateral resistance force and sleeper spacing to be set individually. As a result of performing a reproduction analysis of a full-scale track buckling test, good agreement was obtained.

The rails and sleepers were modelled using beam elements, and the lateral resistance, creepage resistance, and rotational resistance of the rail fastening device were modelled using spring elements. All these spring elements were designed to take nonlinear elasticity into consideration. Both ends of the rail were assumed to be CWR immovable sections, and translational displacement in the y-axis direction was restrained. In this study, only static behaviour due to temperature load is considered, and it is treated as a two-dimensional x-y plane problem.



[a] The whole calculation model



[b] Rails and sleepers

[c] Rail fastening

[d] Ballast resistance

Figure 3: The calculation model for track lateral shift.

The initial lateral imperfection was given by equation (1), and the central vertex was placed at the centre of the analytical model. Note that the initial lateral imperfection gives only the geometric shape, and does not take into account the initial member forces associated with setting this shape.

$$y = \frac{c}{2} \cdot \left(1 + \cos \frac{\pi}{l} x\right) \quad (-l \leq x \leq l) \quad (1)$$

Here, x is the coordinate in the rail direction, with the centre of the model as the origin. y is the lateral displacement of the track, c is the maximum wave height of the initial lateral imperfection, and l is the half wavelength of the initial lateral imperfection (5 m). In this study, other specifications given to the calculation model were that the rail is JIS50N, the rail fastening device is rail clip, and the ballast longitudinal resistance force is set to be 1.5 times the ballast lateral resistance force.

2.3 Method for estimating ballast lateral resistance force

The method for calculating the ballast lateral resistance force used in the model shown in Figure 3 will be described. The ballast lateral resistance force was calculated using the formula obtained by Kataoka et al. in an experiment [3] on the track bed lateral resistance force assuming the gap of sleepers and vibrations during train running.

The characteristics of the ballast lateral resistance force are as shown in equation (2).

$$g = g_0 (y/a + y) \quad (2)$$

Here, g_0 : the final ballast lateral resistance force, a : coefficient when $g = g_0/2$.

In the uplift section, g_0 and a are derived as follows.

$$g_0 = 0.56 g_0^* \quad (3)$$

$$a = a^* + 1.7 u_z + 0.3 \text{ mm} \quad (4)$$

On the other hand, in the section where positive rail seat load acts, these values are expressed as follows.

$$g_0 = (0.80 p + g_0^* / 3) + 0.32 / 3 g_0^* \quad (5)$$

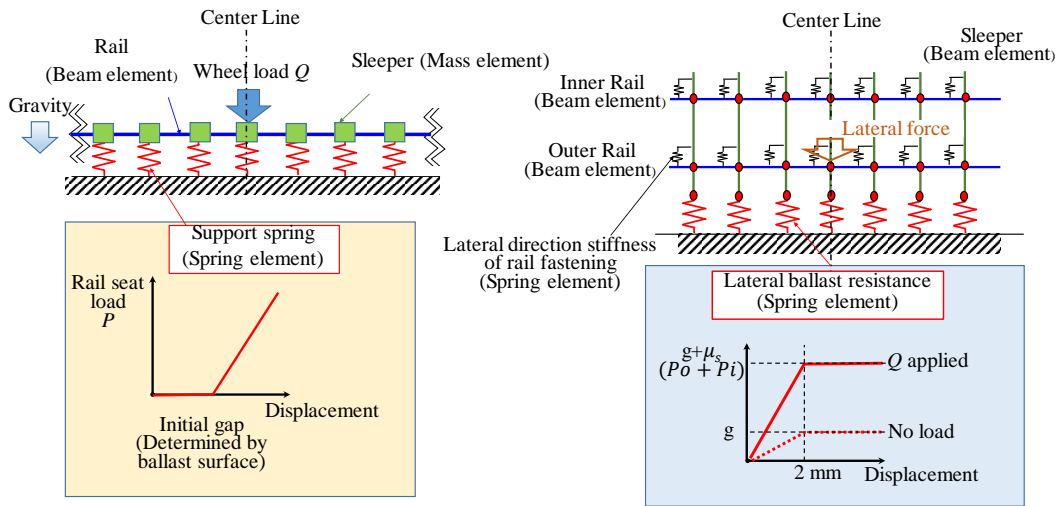
$$a = a^* + 1.8 \quad (6)$$

Here, u_z : gap, p : rail seat load, g_0^* : final ballast lateral resistance force unloaded, a^* : Coefficient when unloaded.

In this study, it is assumed that the centre of one vehicle is at the centre of the analytical model shown in Figure 2 and set the characteristics of the roadbed lateral resistance force. Here, the wheel load is 50kN, the rail support spring coefficient is 20 MN/m per sleeper, the vehicle wheelbase is 2.1m-14.4m-2.1m, a^* is 1 mm, and g_0^* is 5 kN/m/rail.

2.4 Method of examining lateral stability of track against lateral force

The lateral stability of track with unsupported sleepers against lateral force was calculated as follows using the model in Figure 4.



[a] Rail seat load calculation model

[b] Lateral displacement calculation model

Figure 4: The calculation model for lateral stability

First, the rail seat loads are determined using a finite spacing support model [a] based on the wheel load of the running vehicle, and based on that, the ballast lateral resistance force is set accordingly for each sleeper. Here, the ballast lateral resistance

force exerted by the rail seat load is set as follows. The ballast lateral resistance force handled by the sleeper bottom is 1/3 of the total, and this is equivalent to the friction force between the sleeper bottom and the ballast surface top due to the dead load of one sleeper [4]. A coefficient of friction is calculated from this relationship, and the product of this coefficient multiplied by the dead load of the sleepers and the calculated sum of the left and right rail seat loads is taken as the ballast lateral resistance force. The reason why Equations (2) to (6) are not used is because the vibration of the train when running at unsupported sleepers, which is the basis for these equations, is unknown.

Next, using a two-dimensional FEM calculation model [b] in the longitudinal and lateral directions of the track, the response to lateral force is calculated. This calculation model consists of a beam element and a spring element, and the spring element considers slippage due to friction, giving it elastic-plastic properties that keep its rigidity constant when a load above a certain level is applied. Using this model, the lateral axle force at which the sleeper starts to slide was determined.

The track conditions used in this study are narrow gauge tracks with JIS50N rails and PC sleepers (sleeper spacing 650 mm), with continuous unsupported sleepers set at the centre of the calculation model.

3 Results

3.1 The actual state of the track condition at significant misalignments

Table 1 shows the results of surveying the general condition and unsupported sleepers' status of the areas where major misalignments have occurred in recent years. The situation of unsupported sleepers was calculated using the most recent track inspection vehicle data at the time of the event. It is believed that these misalignments were discovered during the process in which track gradually moved laterally due to the balance of forces as the temperature increase. All rails are JIS50N, and the gap are calculated assuming a uniform sleeper spacing of 650 mm. There are continuous unsupported sleepers in all locations. Here, the gap is calculated for both the left and right rails, but the unsupported sleepers are assumed to be unsupported on both sides.

Location	Curve Radius(m)	Superelevation (mm)	Maximum lateral shift (mm)	Rail temperature (°C)	Maximum gap (mm)	Continuous unsupported sleepers (pieces)
1	400	61	53	48	4.8	9
2	820	30	24	51	3.7	8
3	1200	47	19.6	54	6.7	7

Table1: Situation of the location where the significant misalignments occurred

The possible causes of the misalignments are that at location 2, there was a problem with the setting of the rail neutral temperature, and at location 3, the ballast bed had been replaced before the incident occurred. Location 1 is the location shown in Figure1, and the cause was unknown at the time of the event. In this study, analysis was carried out targeting location 1 was targeting location 1, where the event occurred on a sharp curve with low buckling stability, and countermeasures were considered.

3.2 Existence of unsupported sleepers in CWR sections

The existence of unsupported sleepers in CWR sections on representative of commercial lines where JIS 50N rail is installed was investigated. Using data from 3322 continuous unsupported sleeper locations, the relationship between the number of continuous unsupported sleepers and the maximum gap was clarified. The results are shown in Figure 5. This result shows that there is a high correlation between the number of continuous unsupported sleepers and the maximum gaps. The range of the largest continuous unsupported sleeper observed was 6.5 m, and the largest maximum gap was 12.8 mm.

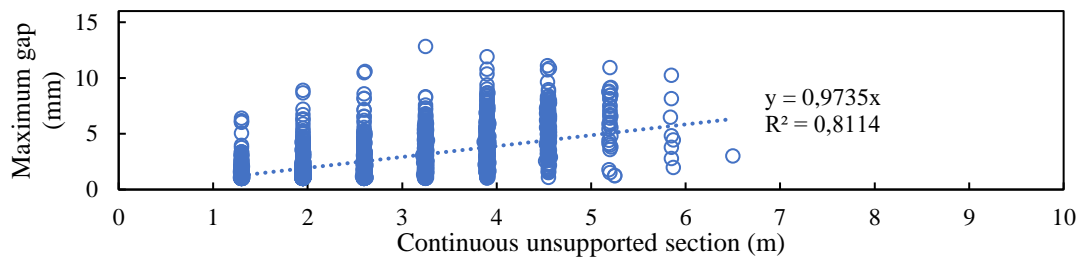


Figure 5: Relationship between continuous unsupported section and the maximum gap.

3.3 Results of examination of lateral stability

Assuming conditions under which a suburban vehicle travels in location 1 in Table 1, the sum of dynamic wheel loads during vehicle travel was calculated to be 117.6 kN using the wheel load estimation equation [5].

To confirm the influence of unsupported sleeper condition on the track lateral shift, two types of maximum gap were determined for each number of continuous unsupported sleepers. They are those calculated using the regression equation shown in Figure 5, and those in the top 10% statistically calculated from Figure 5. The gap for each sleeper was determined by interpolation using trigonometric functions, and the ballast resistance force was set.

Using these unsupported sleeper conditions, and the method shown in Section 2.4, the rail seat load and track response due to lateral axle force were calculated. Figure 6 shows the calculation results of the lateral axle force limit at which the sleepers begin to slip.

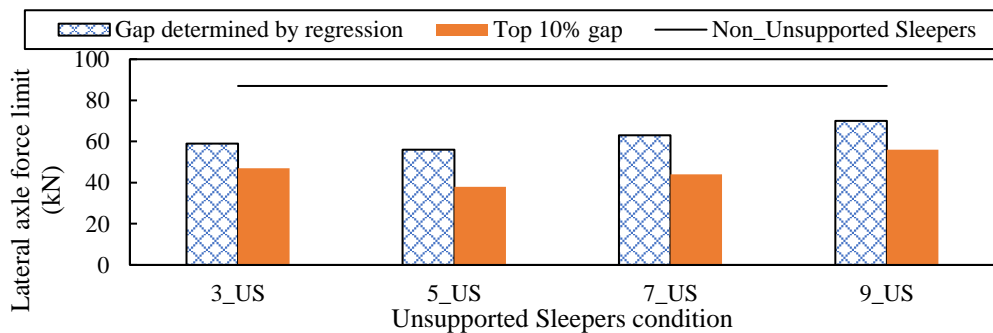


Figure 6: Relationship between unsupported sleeper condition and lateral axle force limit.

This result confirms that the presence of continuous unsupported sleepers reduces the lateral axle force limit, and that for the same number of continuous unsupported sleepers, the larger the gap, the lower the lateral axle force limit. However, there is not much relationship between the number of continuous unsupported sleepers and the lateral axle force limit.

On the other hand, for location 1, the relationship between the lateral track irregularity by 10m chord versine method and the lateral axle force was determined using the lateral force estimation equations [5]. A suburban vehicle was used, and two speeds were investigated: the standard 75km/h and 85km/h. The results are shown in Figure 7. To prevent lateral axle force from exceeding the limit value shown in Figure 6, it is considered desirable to suppress misalignment to about 20 mm.

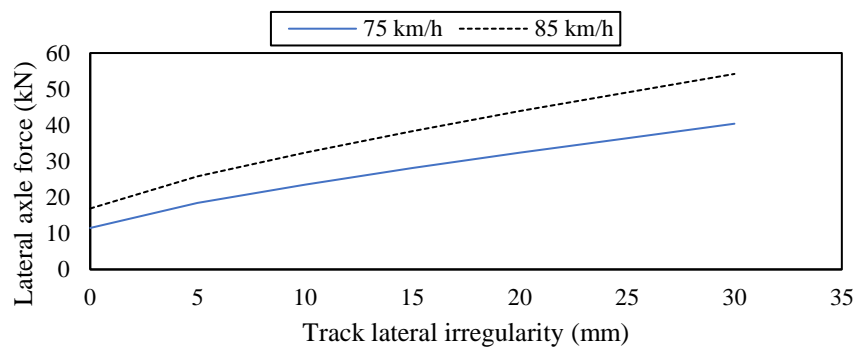


Figure 7: Relationship between track lateral irregularity and lateral axle force

3.4 Temperature increase and track lateral shift

The conditions for the continuous unsupported sleepers were the same as those shown in Section 3.3, and the ballast lateral resistance force was calculated based on these conditions. Figure 8 shows an example of the ballast lateral resistance force characteristics set.

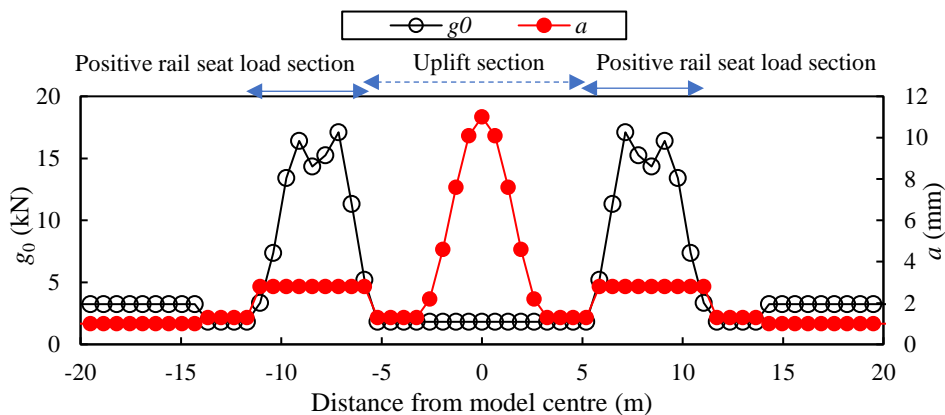


Figure 8: Example of ballast lateral resistance force characteristics

Figure 9 shows the results of calculating the relationship between temperature increase and track lateral misalignment for each number of continuous unsupported sleepers. Here, the horizontal axis shows the sum of the initial lateral imperfection and the lateral displacement due to temperature increase. In addition, breaks in the plot indicate points where the balance calculation was discontinued. The solid line uses the gap calculated using the regression formula, while the broken line uses the gap of the top 10%.

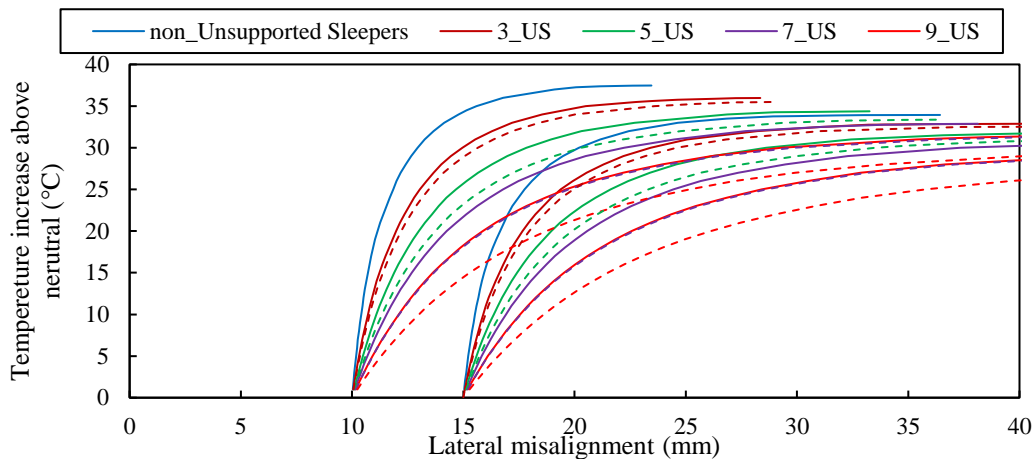


Figure 9: Relationship between rail temperature increases and track lateral shift.

As the number of continuous unsupported sleepers (numbers in the legend) increases, the amount of lateral displacement associated with an increase in temperature increases, and when the initial lateral imperfection is large, the amount of lateral displacement associated with an increase in temperature increases. Further, the larger the gap, the larger the amount of lateral displacement.

Based on the neutral temperature and maximum temperature of the rails actually installed, a temperature increase range of 25 °C was considered as a guideline. To suppress the lateral misalignment to 20 mm, if the initial imperfection is 15 mm, it is necessary to limit the number of continuous unsupported sleepers to 3 or less, but if the initial imperfection is 10 mm, up to 7 continuous unsupported sleepers can be tolerated.

3.5 Proposal of management Standards

Standards were formulated based on the above analysis results. When formulating the standards, consideration was given to ensuring safety standards for prior maintenance, considering that work to loosen the ballast, such as tamping, is prohibited during periods of high rail temperature.

As a result, standards were established for curves with a radius of less than 600 m, where there are seven or more continuous unsupported sleepers, gap is 4 mm or more, and where track lateral irregularity is 10 mm or more, maintenance work must be carried out before the summer season.

Prior to the implementation of the standards, a survey of the target sections within the JR West jurisdiction (612 curves, 175.3 km in length) was conducted, and 19

locations were found to be applicable, and it was confirmed that the number was sufficient to meet the requirements. This standard has been in operation since April 2021, and since then there have been no significant lateral track misalignments in CWR sections with sharp curves, and it is considered to be having a certain degree of effectiveness.

4 Conclusions and Contributions

The findings obtained are shown below.

- Continuous unsupported sleepers were found to exist at all locations where significant lateral track misalignments had occurred in the past.
- It was confirmed that there is a high correlation between the range of continuous unsupported sleepers and the maximum gap.
- It was found that the presence of unsupported sleepers lowers the limit value of lateral axle force that may cause lateral displacement of the track. On the other hand, there was no clear correlation between the number of continuous unsupported sleepers and the limit value of lateral axle force.
- It was found that when the number of continuous unsupported sleepers is large, the amount of lateral displacement of the track increases when the temperature increases.
- Based on the knowledge obtained above, management standards to be applied to CWR sections with sharp curves were formulated. Three years have passed since then, there has been no significant lateral track misalignments.

Acknowledgements

The author would like to take this opportunity to express my gratitude to the excellent researchers at RTRI who participated in discussions and tests regarding the use of unsupported sleepers in this research, and to my colleagues at JR West who discussed the standard development.

References

- [1] M. Kusuda, T. Deshimaru, H. Kataoka, "A study on the design method for the ballasted track in consideration of unsupported sleepers", Proceedings of the International Heavy Haul Association STS Conference, 183-191, 2019.
- [2] D. Yamanoka, M. Kusuda, H. Tanaka, M. Matsumoto, H. Kataoka, "Proposal for Unsupported Sleeper Detection Method and Utilization in Track Maintenance", QR of RTRI, Vol.63, No.1, 2022.
- [3] H. Kataoka, H. Yanagawa, M. Takahara, "An Analysis of the Buckling of Track Reflecting the Vehicle Load", RTRI Report, Vol.17, No.2, 5-10, 2003. (In Japanese.)
- [4] Y.Sato, T.Miyai, "Characteristics of Lateral Ballast Resistance", Quarterly Report of RTRI, Vol.18, No.3, 139, 1977.
- [5] H.Takai, M.Uchida, H.Muramatsu, H.Ishida, "Derailment Safety Evaluation by Analytic Equations", Quarterly Report of RTRI, Vol.43, No.3, 119-124, 2002.